JSLHR

Research Article

Characterizing Swallows From People With Neurodegenerative Diseases Using High-Resolution Cervical Auscultation Signals and Temporal and Spatial Swallow Kinematic Measurements

Cara Donohue,[a] Yassin Khalifa,[b] Shitong Mao,[b] Subashan Perera,[c] Ervin Sejdić,[b,d,e,f] and James L. Coyle[a,g]

Purpose: The prevalence of dysphagia in patients with neurodegenerative diseases (ND) is alarmingly high and frequently results in morbidity and accelerated mortality due to subsequent adverse events (e.g., aspiration pneumonia). Swallowing in patients with ND should be continuously monitored due to the progressive disease nature. Access to instrumental swallow evaluations can be challenging, and limited studies have quantified changes in temporal/spatial swallow kinematic measures in patients with ND. High-resolution cervical auscultation (HRCA), a dysphagia screening method, has accurately differentiated between safe and unsafe swallows, identified swallow kinematic events (e.g., laryngeal vestibule closure [LVC]), and classified swallows between healthy adults and patients with ND. This study aimed to (a) compare temporal/spatial swallow kinematic measures between patients with ND and healthy adults and (b) investigate HRCA's ability to annotate swallow kinematic events in patients with ND. We hypothesized there would be significant differences in temporal/spatial swallow measurements between groups and that HRCA would accurately annotate swallow kinematic events in patients with ND.
Method: Participants underwent videofluoroscopic swallowing studies with concurrent HRCA. We used linear mixed models to compare temporal/spatial swallow measurements (n = 170 ND patient swallows, n = 171 healthy adult swallows) and deep learning machine-learning algorithms to annotate specific temporal and spatial kinematic events in swallows from patients with ND.
Results: Differences ($p < .05$) were found between groups for several temporal and spatial swallow kinematic measures. HRCA signal features were used as input to machine-learning algorithms and annotated upper esophageal sphincter (UES) opening, UES closure, LVC, laryngeal vestibule reopening, and hyoid bone displacement with 66.25%, 85%, 68.18%, 70.45%, and 44.6% accuracy, respectively, compared to human judges' measurements.
Conclusion: This study demonstrates HRCA's potential in characterizing swallow function in patients with ND and other patient populations.

[a]Department of Communication Science and Disorders, School of Health and Rehabilitation Sciences, University of Pittsburgh, PA
[b]Department of Electrical and Computer Engineering, Swanson School of Engineering, University of Pittsburgh, PA
[c]Division of Geriatric Medicine, Department of Medicine, University of Pittsburgh, PA
[d]Department of Bioengineering, Swanson School of Engineering, University of Pittsburgh, PA
[e]Department of Biomedical Informatics, University of Pittsburgh School of Medicine, PA
[f]Intelligent Systems Program, School of Computing and Information, University of Pittsburgh, PA
[g]Department of Otolaryngology, School of Medicine, University of Pittsburgh Medical Center, PA
Correspondence to Cara Donohue: Cad191@pitt.edu
Editor: Michelle Ciucci

Received March 9, 2021
Revision received April 21, 2021
Accepted May 21, 2021
https://doi.org/10.1044/2021_JSLHR-21-00134

Patients with neurodegenerative diseases (ND) are frequently diagnosed with dysphagia at some point during the disease course as motor function progressively deteriorates. In fact, prevalence estimates of dysphagia in patients with ND, such as dementia, multiple sclerosis,

Disclosure: *The authors have declared that no competing financial or nonfinancial interests existed at the time of publication.*

Parkinson's disease (PD), and amyotrophic lateral sclerosis (ALS), range from 13% to 98% (Aghaz et al., 2018; Alagiakrishnan et al., 2013; Easterling & Robbins, 2008; Onesti et al., 2017; Suttrup & Warnecke, 2016). Closely monitoring swallow function throughout the disease course is vital for patients with ND to predict and mitigate adverse outcomes (e.g., malnutrition, dehydration, aspiration pneumonia, and respiratory failure) while simultaneously helping patients maintain quality of life via methods of intake that are safe and align with patient preferences and intake requirements (da Costa Franceschini & Mourão, 2015; Paris et al., 2013; Schwartz, 2018; Smith & Ferguson, 2017). While videofluoroscopic swallowing studies (VFSSs) and fiberoptic endoscopic evaluation of swallowing remain the gold standards for swallowing instrumental assessment methods, they are not always feasible or easily accessible, especially for patients with ND who may have physical mobility impairments, multifactorial health problems, and difficulty attending in-person appointments due to transportation challenges or concerns related to having a compromised immune system (e.g., COVID-19 pandemic; Audag et al., 2019; Waito et al., 2017). Likewise, patients with ND may require frequent reevaluation of swallow function due to the progressive disease nature, day-to-day variability in swallow function, and the inability to fully capture a patient's swallowing ability during instrumental swallow evaluations due to time constraints (i.e., limited clinician availability and need to minimize radiation exposure; Audag et al., 2019). In addition to this, while some research studies have characterized some aspects of swallow function in patients with ND, few studies report objective changes in swallowing based on normative reference data, and furthermore, there is a general lack of consensus regarding specific impairments that occur throughout the disease courses of various ND (Waito et al., 2017). Therefore, the ability to monitor swallow function continuously, remotely, noninvasively, and objectively would be an especially useful innovation for patients with ND as well as clinicians and caregivers of patients with ND.

High-resolution cervical auscultation (HRCA) is a promising, noninvasive, sensor-based dysphagia screening method with potential as a diagnostic adjunct to VFSSs. HRCA autonomously quantifies several aspects of swallowing physiology via acoustic and vibratory signals that are obtained from a contact microphone and a tri-axial accelerometer that are attached to the anterior laryngeal framework during swallowing. Using advanced signal processing and machine-learning techniques, HRCA has classified swallows as safe versus unsafe based on the penetration–aspiration scale (PAS; Dudik et al., 2018; Dudik, Coyle, & Sejdić, 2015; Dudik, Jestrovic, et al., 2015; Dudik, Kurosu, et al., 2015; Jestrović et al., 2013; Robbins et al., 1999; Sejdić et al., 2013; Yu et al., 2019), tracked hyoid bone movement (Donohue et al., 2020; Mao et al., 2019), annotated specific temporal swallow kinematic events (e.g., upper esophageal sphincter [UES] opening, UES closure, laryngeal vestibule closure [LVC], and laryngeal vestibule [LV] reopening; Donohue et al., 2020a; Khalifa et al., 2021a, 2021b; Mao et al., 2021), and classified swallows based on Modified Barium Swallow Impairment Profile scores (Martin-Harris et al., 2008) with similar accuracy as human judges (Donohue et al., 2020, 2020a). Recently, HRCA has demonstrated promise in characterizing swallow function in specific patient populations, including patients after stroke and patients with ND (Donohue et al., 2020b; Kurosu et al., 2019). A preliminary study found that using HRCA signals as input, logistic regression and decision trees classified swallows between patients with ND and age-matched healthy adults with 99% accuracy, 100% sensitivity, and 99% specificity (Donohue et al., 2020b), offering a promising and noninvasive system for early detection of significantly atypical swallow physiology in mildly symptomatic patients who may otherwise evade traditional methods of identification. In this study, we sought to expand upon this prior work, which explored HRCA's capability in classifying (i.e., screening) between swallows from patients with ND and swallows from age-matched healthy adults, with the following aims: (a) compare temporal and spatial swallow kinematic measures between patients with ND and age-matched healthy adults and (b) investigate HRCA's ability to accurately annotate specific swallow kinematic events in patients with ND. We hypothesized that there would be differences in temporal (bolus passes the mandible, hyoid onset, hyoid maximum, hyoid offset, UES opening, UES closure, LVC, and LV reopening) and spatial (hyoid bone displacement and UES anterior–posterior distension) swallow measurements between patients with ND and age-matched healthy adults and that HRCA would accurately annotate temporal and spatial swallow kinematic events in patients with ND.

Method

Participants, Study Procedures, and Equipment

We conducted data analyses on two distinct sets of data collected at two different time points from patients with ND and age-matched healthy community-dwelling adults. All enrolled participants provided written informed consent, and both studies were approved by the appropriate institutional review board. The data set from patients

Table 1. Bolus characteristics for all swallows included in the neurodegenerative patient data set.

Bolus condition	No. of swallows (%)
Thin by spoon	35 (20.59)
Thin by cup	90 (52.94)
Thin by straw	45 (26.47)
Head position	
Chin down	15 (8.82)
Head neutral	155 (91.18)
Swallow type	
Single	29 (17.06)
Sequential	23 (13.53)
Multiple	118 (69.41)

with ND consisted of 170 thin liquid swallows from 20 patients (age range: 35–82 years, M_{age} = 61.25 years, SD = 12.17; 10 men and 10 women). For the patients with ND data set, the mean number of swallows (± SD) per patient was 8.5 (± 4.36), with a range of 2–19 swallows per patient. Bolus characteristics from the swallows used for analyses can be viewed in Table 1. Patients with ND had a variety of diagnoses, including PD, myasthenia gravis, motor neuron disease, multiple sclerosis, muscular dystrophy, ALS, myotonic dystrophy, and progressive muscle weakness not otherwise specified. Patients with ND were referred for VFSSs by their physicians and had volunteered to participate in an ongoing HRCA project and underwent clinician-guided VFSSs with concurrent HRCA as a part of their clinical care due to suspected dysphagia rather than a standardized VFSS for research purposes. In contrast, the data set from the age-matched healthy community-dwelling adults consisted of 171 thin liquid swallows from 51 adults (age range: 39–87 years, M_{age} = 67.21 years, SD = 10.56; 22 men and 29 women). For the healthy swallow data set, the mean number of swallows (± SD) per healthy adult was 3.35 (± 1.68), with a range of one to nine swallows per healthy adult. Bolus characteristics for the swallows used for analyses can be viewed in Table 2. Healthy community-dwelling adults were enrolled based on self-report of absence of the following exclusionary criteria: history of swallowing difficulties, neurological disorder, surgery to the head or neck region, or chance of being pregnant (if female). Healthy participants underwent standardized VFSSs in the lateral plane with concurrent HRCA to minimize radiation exposure (average fluoro time: 0.66 min for 10 swallows). Our standardized VFSS methods are described in detail in previous publications (Donohue et al., 2020, 2020a, 2020b).

Equipment for both research studies included a standard fluoroscopy system (Ultimax System, Toshiba, for the ND patient data collection; Precision 500D System, GE Healthcare, LLC, for the age-matched healthy adult data collection), a frame grabber module for obtaining video segments (AccuStream Express HD, Foresight Imaging), a tri-axial accelerometer (ADXL327, Analog Devices) powered by a power supply with a 3-V output (Model 1504, B&K Precision), and a contact microphone. VFSSs were conducted at a pulse rate of 30 pulses per second. VFSS images and HRCA signals were obtained at a higher sampling rate (60–73 frames per second) according to Shannon's sampling theorem and then later down-sampled to 30 frames per second (Oppenheim et al., 1999). The HRCA sensors (contact microphone and tri-axial accelerometer) were carefully placed on the anterior laryngeal framework with tape in alignment with the participant's neck to obtain the best VFSS images and signals (Dudik, Coyle, & Sejdić, 2015; Takahashi et al., 1994; see Figure 1). Following data collection, acoustic and vibratory signals from the contact microphone and tri-axial accelerometer were bandpass-filtered, amplified (Model P55, Grass Technologies), and digitized via a data acquisition device (National Instruments 6210 DAQ) through the SignalExpress program in LabVIEW (National Instruments) at a sampling rate of 20 kHz.

Table 2. Bolus characteristics for the swallows included in the healthy community-dweller data set.

Bolus condition	No. of swallows (%)
Thin liquid by spoon	78 (45.61)
Thin liquid by cup	93 (54.39)

Note. Thin by spoon swallows were 3 ml, and thin by cup swallows ranged from 5 to 40 ml (M = 16.87 ml).

Temporal and Spatial Swallow Kinematic Analyses

Prior to performing temporal or spatial swallow kinematic measurements and PAS ratings, trained raters underwent inter- and intrarater reliability tests returning intraclass correlation coefficients (ICCs; Shrout & Fleiss, 2005) of at least .9 and percent exact agreement of at least 80%, respectively. Temporal swallow kinematic measurements included the video frames at which the following events occurred: bolus head passes the mandible, onset of maximal hyoid displacement (recently labeled "hyoid burst" in other studies), hyoid reaches maximum displacement, hyoid return to rest, onset of UES opening, onset of UES closure, onset of LVC, and onset of LV reopening. The definition of all temporal swallow kinematic measurements can be viewed in Table 3. Spatial swallow kinematic measurements included distance of hyoid bone displacement and width of anterior–posterior UES distension. The methods used for hyoid frame-by-frame tracking are described in our previous publications (Donohue et al., 2020; Mao et al., 2019; Zhang et al., 2020). The methods used for anterior–posterior UES distension were the same as those in our previous work with the exception of rating three frames per swallow instead of five frames (Shu, 2019; Shu et al., 2021). This was done to increase the efficiency of data analysis since a paired t test revealed nonsignificant differences (p = .363) between three- and five-frame measurements of anterior–posterior UES distention. Spatial swallow kinematic measurements were scaled to an anatomical scalar (length of C2–C4) to control for participant size (Brates et al., 2019; Molfenter & Steele, 2014). Three trained raters completed temporal swallow kinematic measurements with ongoing intrarater reliability within a three-frame tolerance (0.1 s) and ICCs of 1.00 for each event by randomly selecting one swallow to remeasure every 10 swallows. Another trained rater completed interrater reliability for temporal swallow kinematic measurements by randomly selecting and remeasuring 10% of swallows, with ICCs of 1.00. Two trained raters completed spatial swallow kinematic measurements with ongoing intrarater reliability to minimize and control for judgment drift. Intrarater reliability for hyoid frame-by-frame tracking was maintained by randomly remeasuring10 swallows out of every 100 swallows, with average ICCs of .976. Intrarater reliability for anterior–posterior UES distention was maintained by randomly remeasuring

Figure 1. Location of high-resolution cervical auscultation sensors (contact microphone and tri-axial accelerometer) during data collection.

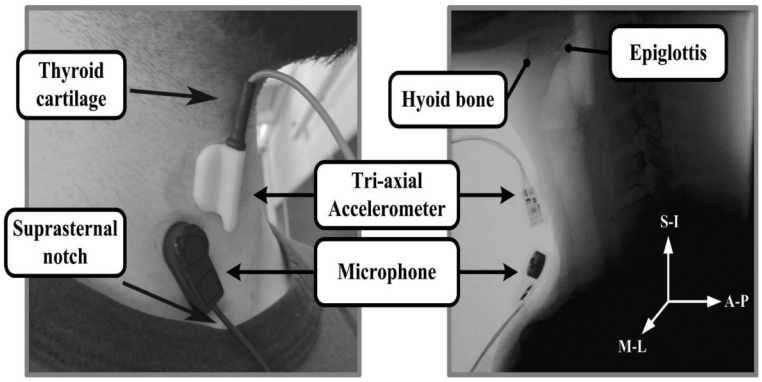

10 swallows out of every 100 swallows, with ICCs of at least .9. Interrater reliability for hyoid frame-by-frame tracking was maintained by randomly remeasuring 10 swallows out of every 100 swallows, with average ICCs of .951. Interrater reliability for anterior–posterior UES distention was completed by another trained rater on 10% of swallows that were randomly selected, with ICCs of at least .9. Two trained raters completed PAS ratings. Intrarater reliability of at least 80% exact agreement was maintained by randomly remeasuring 10% of swallows. Another trained rater remeasured 10% of swallows with interrater reliability of at least 80% exact agreement.

HRCA Signals Preprocessing

Signals from the microphone and the tri-axial accelerometer were down-sampled from an original sampling rate of 20–4 kHz to smooth the transient (high-frequency) noise components. The baseline output from HRCA sensors was recorded prior to data collection in order to model the device noise and filter it out from HRCA signals during the data collection. To perform the filtration process, the device noise of each sensor and axis of acceleration was modeled using an autoregressive process, which was then used to build sensor-specific finite impulse response filters that remove such noise from signals. Afterward, motion artifacts and low-frequency noise were eliminated from all three axes of acceleration using fourth-order least squares spline approximation. Finally, wavelet denoising was performed to enhance the signal quality and reduce the effect of other noise sources. Prior to analyzing the data using the LVC machine-learning algorithm with HRCA signals as input, the channel signals were normalized (Goodfellow et al., 2016). Table 4 summarizes and describes the nine HRCA signal features that were extracted from the contact microphone and the three directions of the tri-axial accelerometer (anterior–posterior, superior–inferior, and medial–lateral) and were used to develop the machine-learning

Table 3. Definitions of temporal swallow kinematic events.

Swallow kinematic event	Definition
Bolus crosses mandible	The first frame in which the organized bolus head first reaches or crosses the plane of the ramus of the mandible and is associated with oral propulsion
Onset of hyoid movement	The first movement of hyoid leading to maximal hyolaryngeal excursion
Maximal hyoid displacement	The first frame in which the hyoid is at its maximally displaced position (superior and anterior) during the pharyngeal phase
Offset of hyoid movement	The first frame in which the hyoid is clear and in a stable position for at least two frames after descent at the end of the swallow (the bolus will typically have passed through the UES)
Laryngeal vestibule closure	The first frame in which no air or barium contrast is seen in the collapsed laryngeal vestibule
Laryngeal vestibule reopening	The first frame in which the laryngeal vestibule reopens
UES opening	The first frame in which separation of the posterior and anterior walls of the UES has begun
UES closure	The first frame in which no column of air or barium contrast is seen separating the posterior and anterior walls of the UES
Swallow reaction time	The time between the bolus crossing the mandible and hyoid onset
Hyoid onset to UES opening	The time between hyoid onset and UES opening
Duration of UES opening	The time between UES opening and UES closure
LVC reaction time	The time between hyoid onset and LVC
LVC duration	The time between LVC and LV reopening

Note. UES = upper esophageal sphincter; LVC = laryngeal vestibule closure; LV = laryngeal vestibule.

Table 4. Features extracted from the high-resolution cervical auscultation (HRCA) signals.

Domain	Signal feature	Meaning of the HRCA signal feature
Time	Standard deviation	Reflects the signal variance around its mean value
	Skewness	Describes the asymmetry of amplitude distribution around mean
	Kurtosis	Describes the "peakness" of the distribution relative to normal distribution
Information–theoretic	Lempel–Ziv complexity	Describes the randomness of the signal
	Entropy rate	Evaluates the degree of regularity of the signal distribution
Frequency	Peak frequency (Hz)	Describes the frequency of maximum power
	Spectral centroid (Hz)	Evaluates the median of the spectrum of the signal
	Bandwidth (Hz)	Describes the range of frequencies of the signal
Time–frequency	Wavelet entropy	Evaluates disorderly behavior for nonstationary signal

algorithms. These HRCA signal features have effectively been used to differentiate between different types of swallows and for extraction of temporal kinematic swallow events (Donohue et al., 2020a, 2020b; Dudik, Coyle, & Sejdić, 2015; Yu et al., 2019).

Data Analyses

To compare the temporal and spatial swallow kinematic measurements from the ND patient data set and the age-matched healthy adults, we fit linear mixed models. To examine differences in hyoid bone displacement based on PAS score for the ND swallows, we fit a linear mixed model. We also fit linear mixed models to examine differences in HRCA signal features associated with maximum anterior–posterior UES distention for swallows from patients with ND and age-matched healthy adults when using features from the entire swallow segment and when using features from the UES opening duration swallow segment.

Machine-Learning Algorithms

Three different previous established machine-learning algorithms using the HRCA signals as input were deployed to annotate the following events using our lab's patient data set (e.g., patients with suspected dysphagia who underwent VFSSs): UES opening onset, UES closure onset, LVC onset, LV reopening onset, and hyoid frame-by-frame tracking (Donohue et al., 2020, 2020a; Khalifa et al., 2021a, 2021b; Mao et al., 2019, 2021; Sabry et al., 2020). We built a convolutional recurrent neural network (CRNN) to estimate UES opening and closure. The CRNN had two convolutional layers, two max pooling layers, three recurrent neural network layers, and four fully connected layers and used the accelerometer signals as input. This CRNN is described in detail in prior publications (Donohue et al., 2020a; Khalifa et al., 2021a, 2021b). To train the CRNN, 10-fold cross validation was used on our lab's entire HRCA patient data set, omitting the swallows from the patients with ND (n = 1,505 swallows). After training the CRNN, we tested its performance on the swallows from patients with ND and calculated the accuracy, sensitivity, and specificity of the CRNN for UES opening and closure compared to human measurements (see Figure 2).

We also built a CRNN to determine LVC and LV reopening. This CRNN was similar to the network described for UES opening and closure, with the exceptions that it had two recurrent neural network layers and three fully connected layers for decision making, and is also described in detail in a prior publication (Mao et al., 2021). The CRNN was trained using 10-fold cross validation on our lab's entire patient data set, omitting the swallows from the patients with ND (n = 885 swallows). After training the CRNN, we tested its performance on the swallows from patients with ND and calculated the accuracy, sensitivity, and specificity of the CRNN for LVC and LV reopening compared to human measurements (see Figure 3).

We built a stacked multilayer recurrent neural network (SRNN) with 10-fold cross validation to predict the location of the body of the hyoid bone on each frame using HRCA signals as input and a bounding box that was 35 × 35 pixels. The methods that were used for HRCA feature extraction and for generating the bounding box have been described in previous publications (see Figure 4; He et al., 2019; Mao et al., 2019; Rebrion et al., 2019). The SRNN was trained using 10-fold cross validation on our lab's entire patient data set of hyoid displacement, omitting the swallows from the patients with ND (n = 400 swallows). After training the SRNN, we tested its performance on a subset of the swallows from patients with ND (n = 88 swallows) and calculated the relative overlapped percentage (ROP) of the bounding boxes for the predicted hyoid bone location based on the CRNN and the ground truth measurement of hyoid bone location based on human judges. ND swallows were excluded from the testing data set because they were part of the original training data set (n = 18 swallows) or because the HRCA signals were corrupted (n = 64 swallows).

Results

Temporal Swallow Kinematic Event Results

Results revealed statistically significant differences ($p < .05$) between swallows from patients with ND and swallows from healthy age-matched adults for hyoid onset to UES opening and duration of UES opening for thin by cup swallows. There were also statistically significant differences ($p < .05$) between the swallows from patients

Figure 2. The evaluation procedure for comparing the accuracy of (a) human measurements of upper esophageal sphincter (UES) opening and closure and (b) the convolutional recurrent neural network (CRNN) measurements of UES opening and closure by (c) calculating the difference between human measurements and the CRNN measurements. TN = true negative; FP = false positive; TP = true positive; FN = false negative.

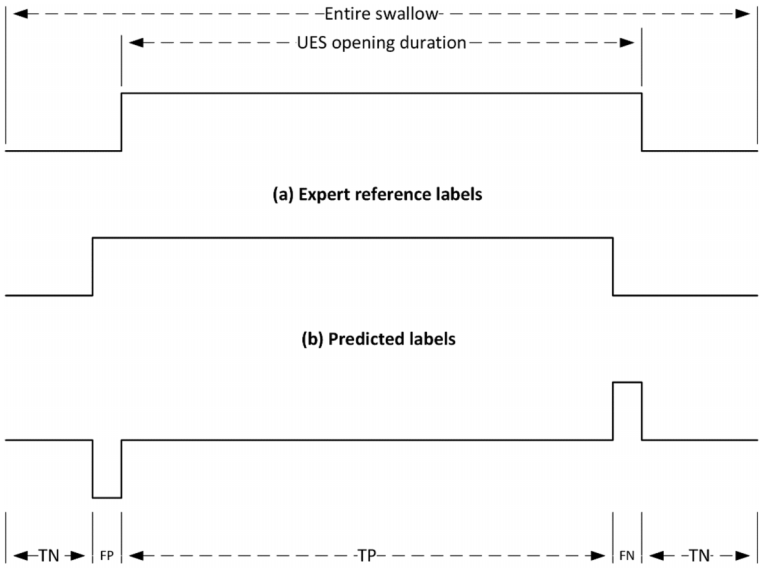

with ND and the swallows from healthy age-matched adults for swallow reaction time, hyoid onset to UES opening, and LVC duration for thin by spoon swallows. A complete summary of the descriptive statistics for the temporal swallow kinematic measurements and the results of the linear mixed model for the patients with ND and the age-matched healthy adults can be viewed in Table 5.

Figure 3. The evaluation procedure for comparing the accuracy of (a) human measurements of laryngeal vestibule closure (LVC) and laryngeal vestibule (LV) reopening and (b) the convolutional recurrent neural network (CRNN) measurements of LVC and LV reopening by (c) calculating the difference between human measurements and the CRNN measurements. TN = true negative; FP = false positive; TP = true positive; FN = false negative.

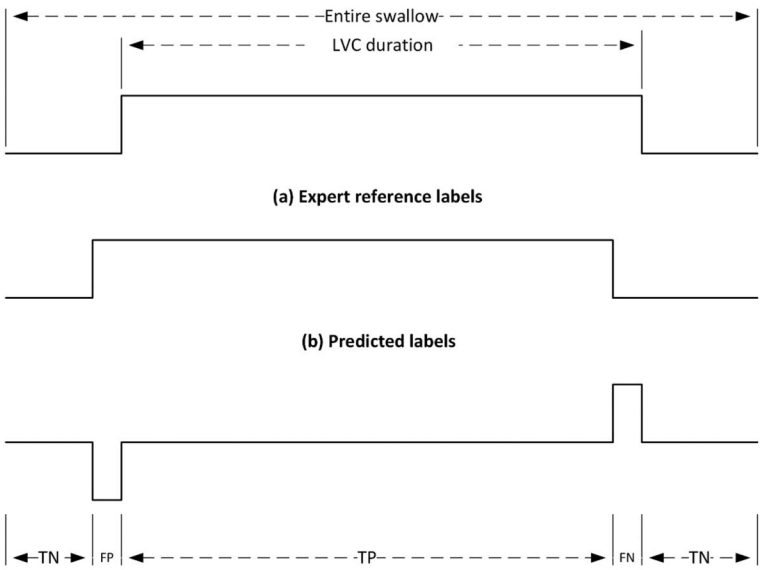

Figure 4. (a) The tracking of the body of the hyoid bone on each frame during a swallow. (b) The relative overlapped percentage of the human-labeled and stacked multilayer recurrent neural network–predicted bounding boxes. (c) The dimensions of the bounding box.

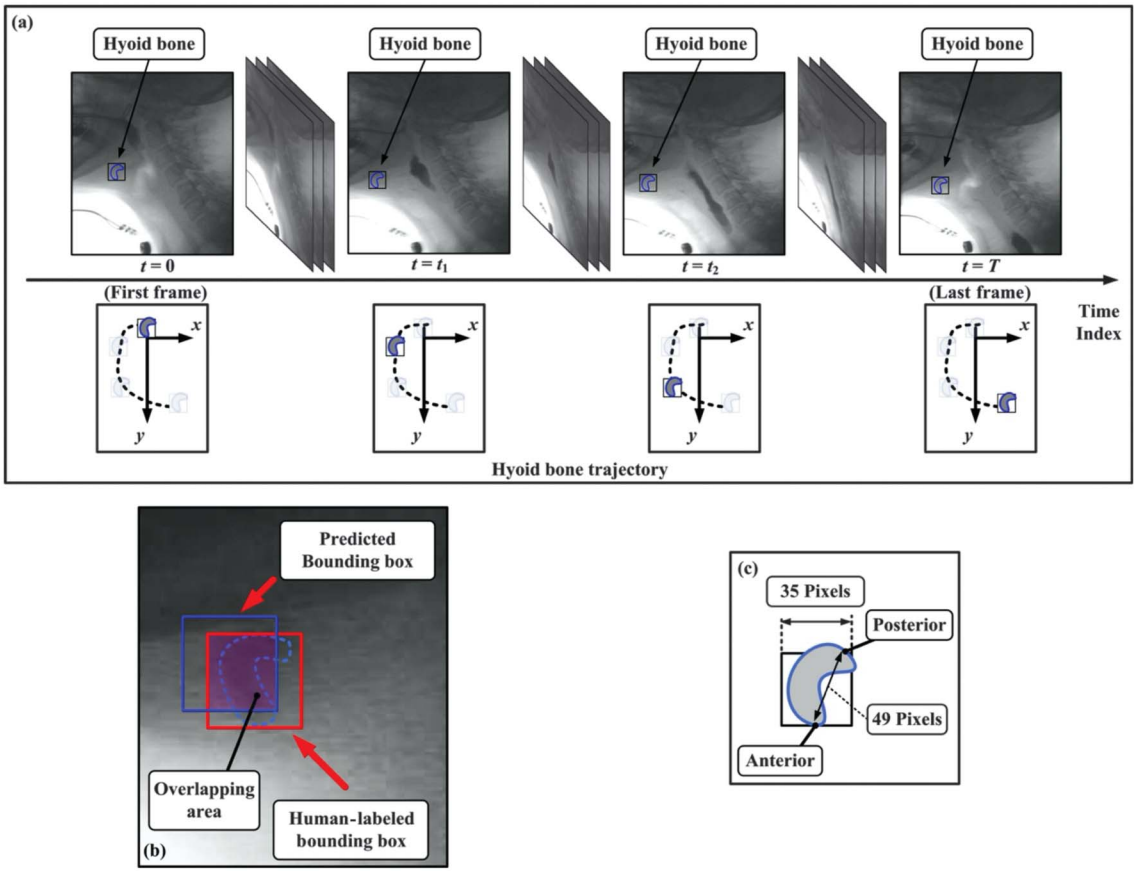

Table 5. Comparison of temporal swallow kinematic measures from the neurodegenerative patient data set and the age-matched healthy community-dwelling adult data set after averaging multiple swallows from the same person using a linear mixed model.

	Neurodegenerative patient data set				Age-matched healthy community-dwelling adult data set				
			95% CI				95% CI		
Temporal swallow kinematic measures	***M***	***SD***	**Lower bound**	**Upper bound**	***M***	***SD***	**Lower bound**	**Upper bound**	***p***
Temporal measure (thin by cup)									
Swallow reaction time	0.094	0.050	0.069	0.119	0.079	0.071	0.057	0.101	.3642
Hyoid onset to UES opening	0.243	0.061	0.214	0.273	0.149	0.058	0.131	0.167	**< .0001***
Duration of UES opening	0.648	0.109	0.596	0.701	0.821	0.100	0.790	0.852	**< .0001***
LVC reaction time	0.408	0.098	0.361	0.456	0.438	0.115	0.403	0.474	.2297
LVC duration	0.384	0.148	0.313	0.456	0.329	0.124	0.291	0.367	.1134
Temporal measure (thin by spoon)									
Swallow reaction time	0.143	0.072	0.094	0.192	0.086	0.117	0.048	0.123	**.0039***
Hyoid onset to UES opening	0.316	0.072	0.267	0.364	0.203	0.061	0.184	0.223	**< .0001***
Duration of UES opening	0.652	0.159	0.545	0.759	0.735	0.114	0.699	0.771	.0544
LVC reaction time	0.430	0.060	0.387	0.472	0.402	0.094	0.372	0.432	.1454
LVC duration	0.456	0.148	0.350	0.562	0.336	0.127	0.296	0.378	**.0026***

Note. Temporal swallow kinematic measures are in seconds. Bold values and asterisks (*) indicate statistical significance, $p < .05$. CI = confidence interval; UES = upper esophageal sphincter; LVC = laryngeal vestibule closure.

Spatial Swallow Kinematic Event Results

Statistically significant differences ($p < .05$) were found between the patients with ND and healthy age-matched adults for superior hyoid bone displacement (normalized to C2–C4) for thin by cup swallows and for anterior and superior hyoid bone displacement (normalized to C2–C4) for thin by spoon swallows (see Table 6). There were also statistically significant differences ($p < .05$) in superior hyoid bone displacement (normalized to C2–C4) for thin by cup swallows when comparing swallows with PAS scores of < 3 versus PAS scores of ≥ 3 (see Table 7). When examining differences in anterior–posterior UES distention between the two groups of swallows, there were no statistically significant differences ($p \geq .05$) in anterior–posterior UES distention after controlling for participant size (see Table 8). In addition to this, there were two statistically significant differences ($p < .05$) in HRCA signal features for thin by cup swallows and 11 statistically significant differences ($p < .05$) in HRCA signal features for thin by spoon swallows associated with maximum anterior–posterior UES distention (normalized to C2–C4) for differentiating swallows from patients with ND and age-matched healthy adults when using features from the entire swallow segment (see Table 9). There were also two statistically significant differences ($p < .05$) in HRCA signal features for thin by cup swallows and 10 statistically significant differences ($p < .05$) in HRCA signal features for thin by spoon swallows associated with maximum anterior–posterior UES distention (normalized to C2–C4) for differentiating swallows from patients with ND and age-matched healthy adults when using features from the UES opening duration swallow segment (see Table 10).

Machine-Learning Algorithm Results

Across the patients with ND data set, the CRNN for UES opening and closure performed with 88.78% accuracy, 91.28% sensitivity, and 86.83% specificity. When comparing the CRNN's accuracy to human measurements, the CRNN annotated UES opening within a three-frame tolerance (0.1 s) for 66.25% of swallows and UES closure for 85.0% of swallows (see Figures 5 and 6). Across the patients with ND data set, the CRNN for LVC and LV reopening performed with 81.03% accuracy, 81.39% sensitivity, and 85.43% specificity. When comparing the CRNN's accuracy to human measurements, the CRNN annotated LVC within a three-frame tolerance (0.1 s) for 68.18% of swallows and LV reopening for 70.45% of swallows (see Figures 7 and 8). When examining the accuracy of the SRNN for hyoid frame-by-frame tracking for the patients with ND data set, the average ROP was 44.6% (± 18.5%) when comparing the performance of the SRNN to human ratings (see Figure 9).

Discussion

This study expanded upon previous preliminary findings that HRCA can accurately differentiate between swallows from the categories "patients with ND" and "age-matched healthy adults" (Donohue et al., 2020b) by illuminating differences in temporal and spatial kinematic swallow measurements between these two groups, revealing differences in HRCA signal features associated with anterior–posterior UES distention between these two groups, and demonstrating HRCA's ability to accurately and more efficiently than human judgment annotate specific temporal swallow kinematic events (UES opening, UES closure, LVC, and LV reopening) and spatial kinematic events (hyoid frame-by-frame tracking) in swallows from patients with ND. While we hypothesized that there would be differences in temporal and spatial swallow kinematic measurements between the swallows from patients with ND and healthy age-matched adults, there were several unexpected findings. For example, patients with ND had greater superior hyoid bone displacement than the age-matched

Table 6. Comparison of mean overall hyoid displacements in pixels and C2–C4 units for thin liquid swallows from the neurodegenerative patient data set and the age-matched healthy community-dwelling adult data set after averaging multiple swallows from the same person using a linear mixed model.

	Neurodegenerative patient data set		Age-matched healthy community-dwelling adult data set		*p*	
Hyoid displacement	**Anterior hyoid**	**Posterior hyoid**	**Anterior hyoid**	**Posterior hyoid**	**Anterior hyoid**	**Posterior hyoid**
Displacements (thin by cup)						
Anterior displacement in pixels	62.85 ± 14.94	59.04 ± 15.25	50.68 ± 10.44	46.66 ± 9.43	**.0008***	**.0008***
Superior displacement in pixels	84.40 ± 22.46	75.50 ± 22.35	60.94 ± 13.75	52.09 ± 11.66	**< .0001***	**< .0001***
Anterior displacement in C2–C4 units	0.46 ± 0.19	0.42 ± 0.16	0.42 ± 0.10	0.39 ± 0.08	.3911	.3001
Superior displacement in C2–C4 units	0.61 ± 0.24	0.54 ± 0.21	0.50 ± 0.10	0.43 ± 0.10	**.0136***	**< .0038***
Displacements (thin by spoon)						
Anterior displacement in pixels	52.59 ± 10.32	45.96 ± 12.52	51.33 ± 10.95	48.24 ± 11.65	.6763	.6219
Superior displacement in pixels	74.69 ± 29.19	69.49 ± 27.18	57.49 ± 13.80	48.55 ± 10.15	**.0096***	**.0003***
Anterior displacement in C2–C4 units	0.38 ± 0.07	0.33 ± 0.08	0.43 ± 0.10	0.40 ± 0.10	.1377	**.0283***
Superior displacement in C2–C4 units	0.54 ± 0.20	0.50 ± 0.18	0.48 ± 0.09	0.40 ± 0.07	.1767	**.0145***

Note. Bold values and asterisks (*) indicate statistical significance, $p < .05$.

Table 7. Comparison of mean overall hyoid displacements in pixels and C2–C4 units for thin liquid swallows from the neurodegenerative patient data set based on penetration–aspiration scale (PAS) scores after averaging multiple swallows from the same person using a linear mixed model.

Hyoid displacement	Neurodegenerative patient data set		
	PAS 1–2	PAS 3–8	*p*
Displacements (thin by cup)			
Maximum anterior displacement in pixels of the anterior hyoid	61.59 ± 12.21	62.38 ± 26.65	.0940
Maximum anterior displacement in pixels of the posterior hyoid	58.11 ± 14.83	54.48 ± 17.88	.7424
Superior displacement in pixels of the anterior hyoid	84.48 ± 24.10	80.83 ± 32.86	**.0004***
Superior displacement in pixels of the posterior hyoid	75.77 ± 24.44	69.38 ± 28.02	**.0005***
Anterior displacement in C2–C4 units of the anterior hyoid	0.42 ± 0.08	0.52 ± 0.35	.0523
Anterior displacement in C2–C4 units of the posterior hyoid	0.40 ± 0.09	0.45 ± 0.26	.9823
Superior displacement in C2–C4 units of the anterior hyoid	0.58 ± 0.16	0.66 ± 0.41	**.0009***
Superior displacement in C2–C4 units of the posterior hyoid	0.52 ± 0.15	0.57 ± 0.35	**.0038***
Displacements (thin by spoon)			
Maximum anterior displacement in pixels of the anterior hyoid	51.43 ± 15.40	49.95 ± 6.60	.6774
Maximum anterior displacement in pixels of the posterior hyoid	44.41 ± 16.97	47.55 ± 8.87	.9492
Superior displacement in pixels of the anterior hyoid	76.37 ± 29.25	71.99 ± 31.46	.6226
Superior displacement in pixels of the posterior hyoid	70.93 ± 27.51	65.21 ± 25.40	.6515
Anterior displacement in C2–C4 units of the anterior hyoid	0.37 ± 0.11	0.42 ± 0.14	.6428
Anterior displacement in C2–C4 units of the posterior hyoid	0.31 ± 0.11	0.40 ± 0.16	.5179
Superior displacement in C2–C4 units of the anterior hyoid	0.56 ± 0.22	0.55 ± 0.16	.5039
Superior displacement in C2–C4 units of the posterior hyoid	0.52 ± 0.21	0.51 ± 0.14	.5510

Note. Bold values and asterisks (*) indicate statistical significance, $p < .05$.

healthy adults for thin by cup and thin by spoon swallows. Interestingly, when comparing the ND swallows with PAS scores of < 3 to the ND swallows with PAS scores of ≥ 3, the swallows with PAS scores of ≥ 3 also had greater superior hyoid bone displacement than the swallows with PAS scores of < 3 for thin by cup swallows, indicating a potential compensatory adaptation in the patients with ND.

It is important to highlight the accuracy and efficiency of the machine-learning algorithms that were implemented in this study. When comparing the efficiency of the CRNN for UES opening and closure to human judges, the CRNN can analyze 150 swallows in approximately 42 s. This would take a human judge approximately 2 min to code UES opening and closure per swallow for 150 swallows for a total of 5 hr. While a clinician may not make this many measurements of UES opening and closure at once, an average VFSS may contain 20 swallows and would take 40 min for a clinician to code in order to fully evaluate UES opening. Availability of rapid measurement of such discrete data from a VFSS examination may provide clinicians with more objective summaries of overall function as opposed to many traditional metrics such as widest or narrowest opening over the course of an examination. Therefore, while HRCA is not meant to replace VFSSs, it may have clinical utility as a diagnostic adjunct by enabling clinicians to receive from the HRCA system objective estimates of swallow function that closely align with human judgment with increased efficiency.

These findings contribute substantively to the limited body of research characterizing swallow function in patients with ND by providing objective, quantitative temporal and spatial measurements of swallowing compared to normative reference values from age-matched healthy adults (Waito et al., 2017, 2020). Likewise, despite the limited number of swallows from patients with ND ($n = 170$), the machine-learning algorithms achieved remarkably high accuracy

Table 8. Comparison of anterior–posterior upper esophageal sphincter (UES) distention maximum width from the neurodegenerative patient data set and the age-matched healthy community-dwelling adult data set after averaging multiple swallows from the same person using a linear mixed model.

Anterior–posterior UES distention	ND patient data set		Healthy adult data set		
	M	*SD*	*M*	*SD*	*p*
Anterior–posterior UES distention (thin by cup)					
Maximum width in pixels	47.53	13.20	41.01	10.16	**.0378***
Maximum width normalized to C2–C4 length	0.34	0.11	0.34	0.09	.9067
Anterior–posterior UES distention (thin by spoon)					
Maximum width in pixels	35.04	6.59	34.56	7.30	.8453
Maximum width normalized to C2–C4 length	0.26	0.05	0.29	0.07	.0970

Note. Bold values and asterisks (*) indicate statistical significance, $p < .05$. ND = neurodegenerative disease.

Table 9. Summary of the differences in high-resolution cervical auscultation signal features associated with maximum anterior–posterior upper esophageal sphincter distention (normalized to C2–C4 length) for swallows from patients with neurodegenerative diseases and age-matched healthy adults when using features from the entire swallow segment.

HRCA signal features	*SD*	Skewness	Kurtosis	Lempel–Ziv complexity	Entropy rate	Peak frequency	Spectral centroid	Bandwidth	Wavelet entropy
Microphone	*ns*	*ns*	*ns*	*ns*	*ns*	*ns*	*ns*	*ns*	*ns*
Anterior–posterior	*ns*	*ns*	*ns* **(0.0258*)**	**0.0195*** **(0.0061*)**	*ns*	*ns*	*ns* **(0.0234*)**	**0.0275*** **(0.0027*)**	*ns* **(0.0381*)**
Superior–inferior	*ns*	*ns*	*ns*	*ns* **(0.0045*)**	*ns*	*ns*	*ns* **(0.0286*)**	*ns* **(0.0078*)**	*ns*
Medial–lateral	*ns*	*ns*	*ns* **(0.0084)**	*ns*	*ns*	*ns*	*ns* **(0.0152*)**	*ns* **(0.0188)**	*ns*

Note. Bold values indicate $p < .05$. HRCA = High-resolution cervical auscultation; *ns* = not significant.
*$p < .05$, thin by cup swallows (thin by spoon swallows).

for annotating temporal kinematic events within a three-frame (0.1 s) human error tolerance level (66%–85% of swallows), which has been cited as acceptable (Lof & Robbins, 1990; Molfenter & Steele, 2013; Robbins et al., 1992). Likewise, the ROP of the machine-learning algorithm and human ratings for tracking hyoid bone displacement was similar to that in previous studies (approximately 50%, range: 45%–57.6%) despite the small number of swallows available for analysis ($n = 88$; Donohue et al., 2020; Mao et al., 2019). This is especially impressive given how small of a structure the hyoid bone is (Loth et al., 2015; Ramagalla et al., 2014) and when considering that the ROP between human raters for hyoid frame-by-frame tracking is only approximately 79% (Donohue et al., 2020; Mao et al., 2019). The marginally reduced accuracy of the SRNN for hyoid tracking for the ND data set may have resulted from the ND swallows having characteristics that were not sufficiently represented in the swallows that were used during the training data set. The accuracy of the algorithms with a relatively small data set may underscore the ubiquity of kinematic swallowing impairments occurring in people with various ND. The ability to monitor swallow function in patients with ND using a noninvasive, portable device that provides continuous, discrete information about swallowing physiology would be a useful and cutting-edge dysphagia early identification and monitoring system for dysphagia management of patients with ND and other patient populations.

The value of early identification of swallowing impairments in patients with ND cannot be underscored. HRCA's ability to classify between swallows from patients with ND and swallows from healthy adults provides preliminary evidence regarding its potential in determining dysphagia screening cutoffs to assist in identifying patients who would benefit from instrumental swallow evaluations and/or implementation of therapeutic interventions that may prolong function and quality of life (Plowman et al., 2016, 2019; Robison et al., 2018; Tabor-Gray et al., 2016; Troche et al., 2010). While the results from this preliminary study are promising, future studies should expand upon this work by investigating HRCA's ability to differentiate and characterize swallows in specific diagnostic categories of ND (e.g., ALS and PD), to differentiate between various patient populations (e.g., ND vs. patients after stroke vs. patients post lung transplant), and to characterize swallows across bolus conditions (e.g., viscosity and volume). In addition to this, it would be advantageous to track changes in temporal and spatial swallow kinematic measurements in patients with ND longitudinally to determine changes

Table 10. Summary of the differences in high-resolution cervical auscultation signal features associated with maximum anterior–posterior upper esophageal sphincter (UES) distention (normalized to C2–C4 length) for swallows from patients with neurodegenerative diseases and age-matched healthy adults when using features from the UES opening duration swallow segment.

HRCA signal features	*SD*	Skewness	Kurtosis	Lempel–Ziv complexity	Entropy rate	Peak frequency	Spectral centroid	Bandwidth	Wavelet entropy
Microphone	*ns*	*ns*	*ns*	*ns*	*ns*	*ns*	*ns*	*ns*	*ns*
Anterior–posterior	*ns*	*ns*	*ns* **(0.0487*)**	**0.0281*** **(0.0128*)**	0.2413 **(0.0215*)**	*ns*	*ns*	*ns*	*ns*
Superior–inferior	*ns*	*ns*	*ns* **(0.0047*)**	*ns* **(0.0031*)**	*ns*	*ns*	*ns* **(0.0285*)**	**0.0418*** **(0.0105*)**	*ns*
Medial–lateral	*ns*	*ns*	*ns*	*ns*	*ns* **(0.0269*)**	*ns*	*ns* **(0.0401*)**	*ns*	*ns* **(0.0188*)**

Note. Bold values indicate $p < .05$. HRCA = High-resolution cervical auscultation; *ns* = not significant.
*$p < .05$, thin by cup swallows (thin by spoon swallows).

Figure 5. Accuracy of the convolutional recurrent neural network (CRNN) for detecting upper esophageal sphincter (UES) opening within a three-frame tolerance (0.1 s) compared to human measurements of UES opening for the neurodegenerative patient data set. VFSS = videofluoroscopic swallowing study.

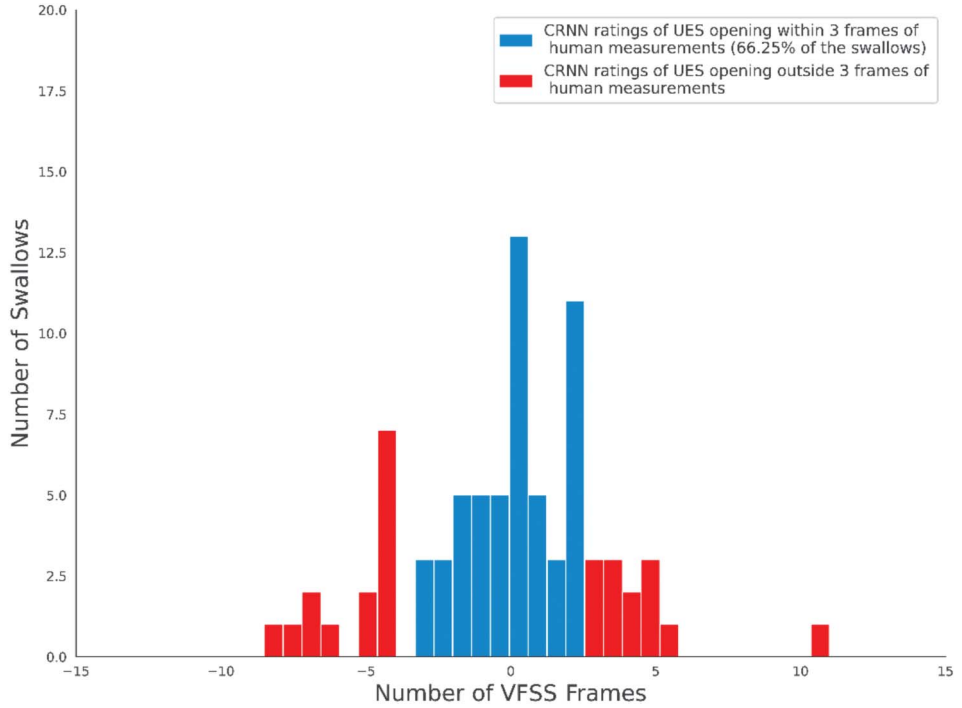

Figure 6. Accuracy of the convolutional recurrent neural network (CRNN) for detecting upper esophageal sphincter (UES) closure within a three-frame tolerance (0.1 s) compared to human measurements of UES closure for the neurodegenerative patient data set. VFSS = videofluoroscopic swallowing study.

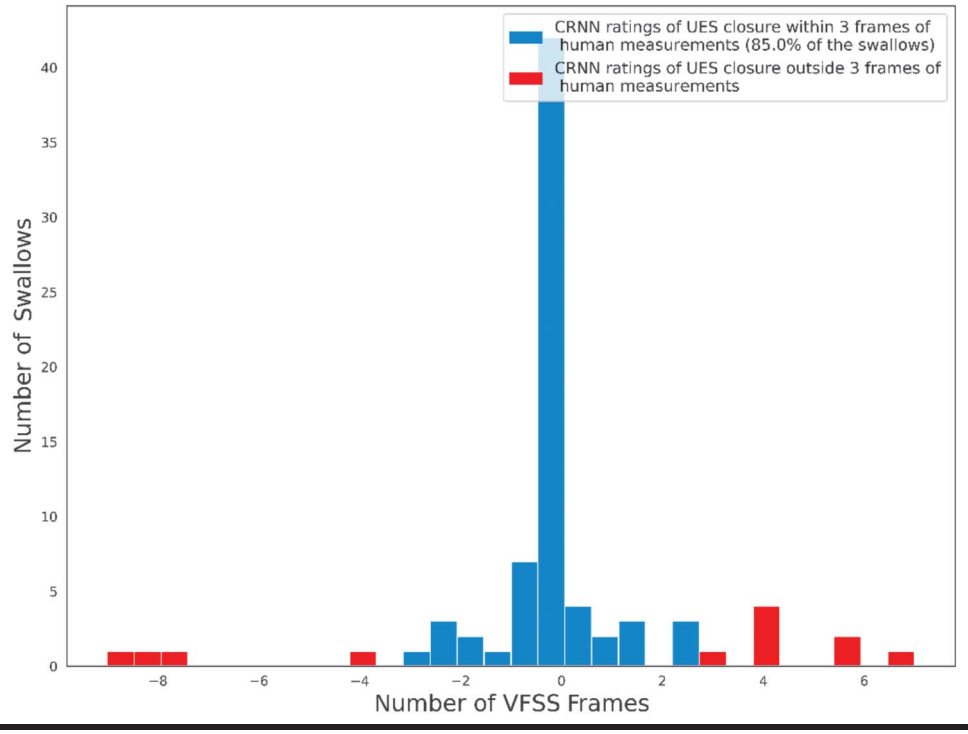

Figure 7. Accuracy of the convolutional recurrent neural network (CRNN) for detecting laryngeal vestibule closure (LVC) within a three-frame tolerance (0.1 s) compared to human measurements of LVC for the neurodegenerative patient data set. VFSS = videofluoroscopic swallowing study.

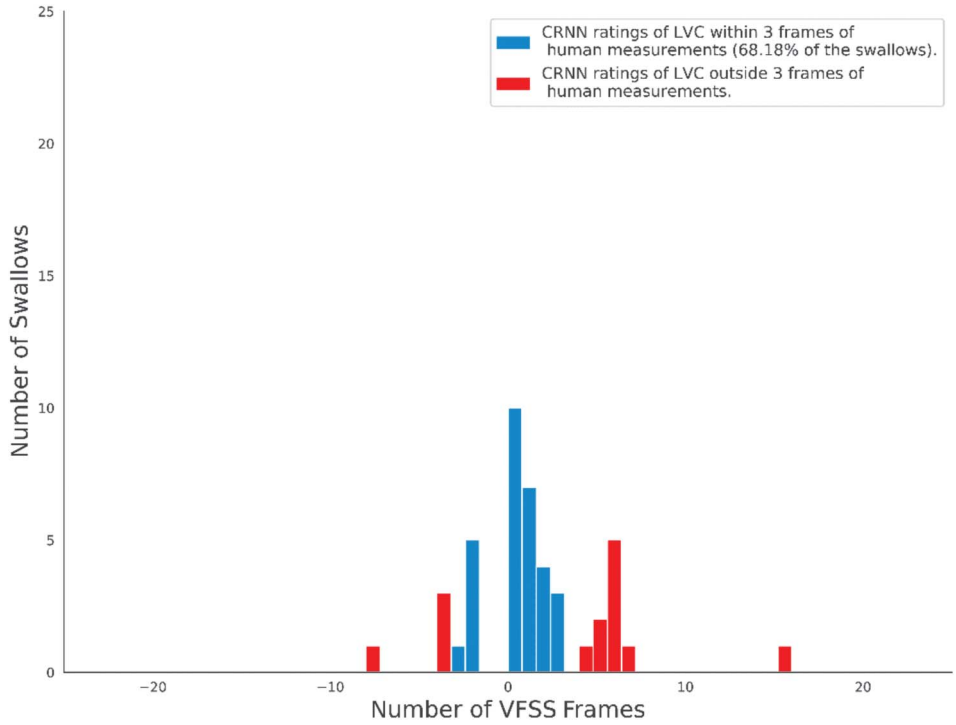

Figure 8. Accuracy of the convolutional recurrent neural network (CRNN) for detecting laryngeal vestibule (LV) reopening within a three-frame tolerance (0.1 s) compared to human measurements of LV reopening for the neurodegenerative patient data set. VFSS = videofluoroscopic swallowing study.

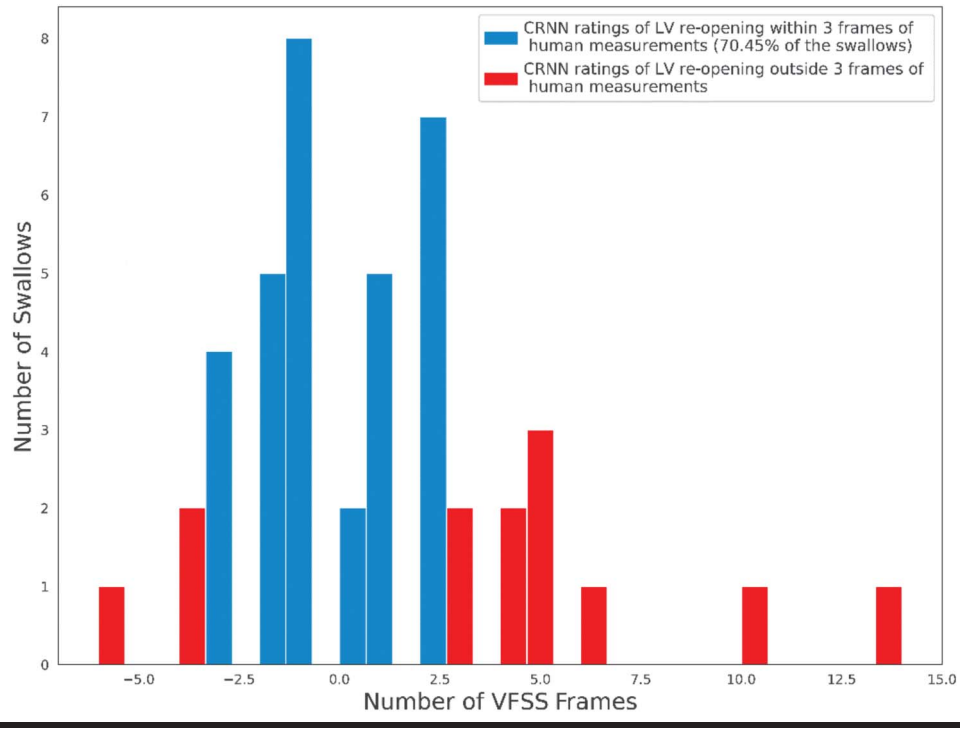

Figure 9. (a) Relative overlapped percentage (ROP) of the human-labeled and stacked multilayer recurrent neural network (SRNN)–predicted bounding boxes across the 10 groups of training data and the testing data set (the neurodegenerative disease swallows). (b) Two examples of the ROP of the human-labeled and SRNN-predicted bounding boxes.

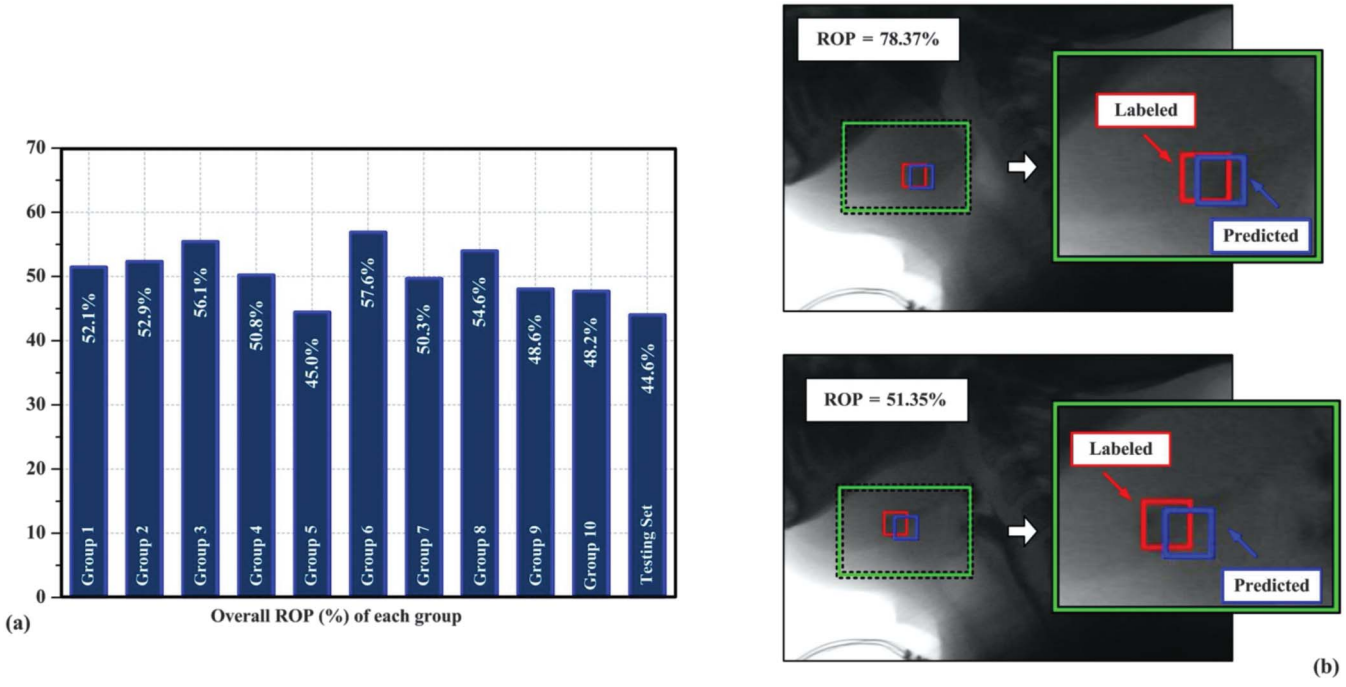

associated with disease progression and severity and to determine whether HRCA can detect subtle changes in swallow function that occur over time. For example, similar to pulmonary function tests, which are frequently used to determine disease progression over time in patients with ND, HRCA may have potential in measuring disease progression and severity related to dysphagia in patients with ND over time. Likewise, future studies should determine HRCA's utility in dysphagia treatment, in addition to its capability as a dysphagia screening and diagnostic adjunct to VFSSs. For example, it would be beneficial to determine HRCA's ability to monitor swallow function in patients with ND over the course of a meal to denote decompensation leading to necessary changes in meal duration and frequency or to provide real-time biofeedback during dysphagia treatment sessions while patients performed compensatory maneuvers (e.g., effortful swallow, Mendelsohn maneuver). Although the machine-learning algorithms performed with exceptional accuracy, it will be important to replicate this research study by including a larger number of swallows with variable bolus conditions and patient characteristics to further improve the robustness of the CRNNs and SRNN.

Limitations

While we attempted to control for confounding variables in this study (e.g., only using thin liquid by cup and 3-ml spoon swallows for analyses), we would like to acknowledge that we used different methods of data collection for the swallows from the patients with ND and the swallows from the age-matched healthy adults. The patients with ND underwent VFSSs as a part of their clinical care, while the age-matched healthy adults underwent standardized VFSSs to minimize radiation exposure. In addition to this, only thin liquid swallows were used for analyses in this study because the standardized VFSS protocol for the age-matched healthy adults only included thin liquid boluses. Future studies should compare temporal and spatial swallow kinematic measurements in patients with ND versus age-matched healthy adults across a variety of bolus conditions (e.g., viscosity and volume) and should explore the ability of the machine-learning algorithms to characterize temporal and spatial swallow kinematic events across bolus conditions. We also investigated a broad, heterogeneous class of patients with ND due to the limited number of patients with specific ND within our swallowing database to ensure that we included enough swallows for analyses (n = 170). That said, our aim was to determine whether classification between a broad category of "people with ND that commonly cause dysphagia" and healthy swallows was feasible with HRCA. Future studies should further characterize swallow function and the accuracy of these machine-learning algorithms in ND based on individual disease diagnosis (e.g., ALS and PD). Likewise, it will be important to replicate this work using a larger number of swallows from patients who are at different stages of disease progression and with varying degrees of dysphagia severity. An additional limitation that is important to note is related

to signal corruption that occasionally occurs during data collection due to uncontrollable technical difficulties that can result from using a complex synchronous VFSS and HRCA setup that increases liability for hardware failures. In this study, signal corruption resulted in some swallows (n = 64) being excluded for analyses with the hyoid frame-by-frame tracking machine-learning algorithm. Finally, we would like to acknowledge several clinical barriers to implementing HRCA currently. While we are enthusiastic about the future potential of using HRCA as a dysphagia screening tool and diagnostic adjunct to VFSSs, it is not yet commercially available for clinicians to purchase and use within clinical settings. Our research lab is in the process of miniaturizing the HRCA system and finalizing the machine-learning algorithms for use within clinical settings. Given that the HRCA system uses inexpensive hardware materials such as a contact microphone and an accelerometer, we are confident that clinicians will be able to purchase a portable version of the system at an affordable price. Additionally, we plan to design the portable HRCA system to interface with common devices such as tablets or smart phones, so that clinicians can receive the HRCA results of the examination from the autonomous machine-learning algorithms for use in interpreting VFSSs.

Conclusions

This study found several differences in temporal and spatial swallow kinematic measurements between patients with ND and age-matched healthy adults, highlighting important changes that occur throughout the progressive courses of these conditions. Additionally, this study found differences in HRCA signal features associated with anterior–posterior UES distention between groups and that using HRCA signals as input to several machine-learning algorithms could accurately annotate UES opening and closure (88.78% accuracy, 91.28% sensitivity, and 86.83% specificity), LVC and LV reopening (81.03% accuracy, 81.39% sensitivity, and 85.43% specificity), and hyoid bone displacement (ROP = 44.6%) in swallows from patients with ND. This provides further evidence regarding HRCA's utility in characterizing swallow function in specific patient populations for dysphagia screening and assessment purposes. These preliminary results suggest that HRCA has considerable future potential as an ongoing dysphagia monitoring system that can provide noninvasive, real-time feedback regarding swallow function to mitigate adverse events in patients with dysphagia.

Compliance With Ethical Standards

All procedures performed in studies involving human participants were in accordance with the ethical standards of the institutional and/or national research committee and with the 1964 Helsinki Declaration and its later amendments or comparable ethical standards.

Informed consent was obtained from all individual participants included in the study.

Acknowledgments

Research reported in this publication was supported by the Eunice Kennedy Shriver National Institute of Child Health and Human Development of the National Institutes of Health under Award R01HD092239, while the data were collected under Award R01HD074819. This study was also supported in part through funding received from the SHRS Research Development Fund, the Audrey Holland Endowed Research Award, and the SHRS PhD Student Award from the School of Health and Rehabilitation Sciences at the University of Pittsburgh. The content is solely the responsibility of the authors and does not necessarily represent the official views of the National Institutes of Health or the University of Pittsburgh. This research study was a part of Cara Donohue's dissertation work. She is grateful for the support and guidance of the other members of her dissertation committee, including David Lacomis, Kendrea L. (Focht) Garand, and Leah Helou. Thanks are also due to Libby Bryson, Tara Smyth, and Dan Kachnycz for their assistance with data collection and coding.

References

Aghaz, A., Alidad, A., Hemmati, E., Jadidi, H., & Ghelichi, L. (2018). Prevalence of dysphagia in multiple sclerosis and its related factors: Systematic review and meta-analysis. *Iranian Journal of Neurology, 17*(4), 180–188. https://doi.org/10.18502/ijnl.v17i4.592

Alagiakrishnan, K., Bhanji, R. A., & Kurian, M. (2013). Evaluation and management of oropharyngeal dysphagia in different types of dementia: A systematic review. *Archives of Gerontology and Geriatrics, 56*(1), 1–9. https://doi.org/10.1016/j.archger.2012.04.011

Audag, N., Goubau, C., Toussaint, M., & Reychler, G. (2019). Screening and evaluation tools of dysphagia in adults with neuromuscular diseases: A systematic review. *Therapeutic Advances in Chronic Disease, 10,* 2040622318821622. https://doi.org/10.1177/2040622318821622

Brates, D., Steele, C. M., & Molfenter, S. M. (2019). Measuring hyoid excursion across the life span: Anatomical scaling to control for variation. *Journal of Speech, Language, and Hearing Research, 63*(1), 125–134. https://doi.org/10.1044/2019_JSLHR-19-00007

da Costa Franceschini, A., & Mourão, L. F. (2015). Dysarthria and dysphagia in amyotrophic lateral sclerosis with spinal onset: A study of quality of life related to swallowing. *NeuroRehabilitation, 36*(1), 127–134. https://doi.org/10.3233/NRE-141200

Donohue, C., Khalifa, Y., Perera, S., Sejdić, E., & Coyle, J. L. (2020a). How closely do machine ratings of duration of UES opening during videofluoroscopy approximate clinician ratings using temporal kinematic analyses and the MBSImP? *Dysphagia,* 1–12. https://doi.org/10.1007/s00455-020-10191-2

Donohue, C., Khalifa, Y., Perera, S., Sejdić, E., & Coyle, J. L. (2020b). A preliminary investigation of whether HRCA signals can differentiate between swallows from healthy people and swallows from people with neurodegenerative diseases. *Dysphagia,* 1–9. https://doi.org/10.1007/s00455-020-10177-0

Donohue, C., Mao, S., Sejdić, E., & Coyle, J. L. (2020). Tracking hyoid bone displacement during swallowing without videofluoroscopy using machine learning of vibratory signals.

Dysphagia, 36, 259–269. https://doi.org/10.1007/s00455-020-10124-z

Dudik, J. M., Coyle, J. L., El-Jaroudi, A., Mao, Z.-H., Sun, M., & Sejdić, E. (2018). Deep learning for classification of normal swallows in adults. *Neurocomputing, 285,* 1–9. https://doi.org/10.1016/j.neucom.2017.12.059

Dudik, J. M., Coyle, J. L., & Sejdić, E. (2015). Dysphagia screening: Contributions of cervical auscultation signals and modern signal-processing techniques. *IEEE Transactions on Human-Machine Systems, 45*(4), 465–477. https://doi.org/10.1109/THMS.2015.2408615

Dudik, J. M., Jestrović, I., Luan, B., Coyle, J. L., & Sejdić, E. (2015). A comparative analysis of swallowing accelerometry and sounds during saliva swallows. *Biomedical Engineering Online, 14*(1), Article 3. https://doi.org/10.1186/1475-925X-14-3

Dudik, J. M., Kurosu, A., Coyle, J. L., & Sejdić, E. (2015). A comparative analysis of DBSCAN, K-means, and quadratic variation algorithms for automatic identification of swallows from swallowing accelerometry signals. *Computers in Biology and Medicine, 59,* 10–18. https://doi.org/10.1016/j.compbiomed.2015.01.007

Easterling, C. S., & Robbins, E. (2008). Dementia and dysphagia. *Geriatric Nursing, 29*(4), 275–285. https://doi.org/10.1016/j.gerinurse.2007.10.015

Goodfellow, I., Bengio, Y., Courville, A., & Bengio, Y. (2016). *Deep learning* (Vol. 1). MIT Press.

He, Q., Perera, S., Khalifa, Y., Zhang, Z., Mahoney, A. S., Sabry, A., Donohue, C., Coyle, J. L., & Sejdić, E. (2019). The association of high resolution cervical auscultation signal features with hyoid bone displacement during swallowing. *IEEE Transactions on Neural Systems and Rehabilitation Engineering, 27*(9), 1810–1816. https://doi.org/10.1109/TNSRE.2019.2935302

Jestrović, I., Dudik, J. M., Luan, B., Coyle, J. L., & Sejdić, E. (2013). Baseline characteristics of cervical auscultation signals during various head maneuvers. *Computers in Biology and Medicine, 43*(12), 2014–2020. https://doi.org/10.1016/j.compbiomed.2013.10.005

Khalifa, Y., Donohue, C., Coyle, J. L., & Sejdić, E. (2021a). On the robustness of high-resolution cervical auscultation–based detection of upper esophageal sphincter opening duration in diverse populations. In *Big Data III: Learning, analytics, and applications*. International Society for Optics and Photonics.

Khalifa, Y., Donohue, C., Coyle, J. L., & Sejdić, E. (2021b). Upper esophageal sphincter opening segmentation with convolutional recurrent neural networks in high resolution cervical auscultation. *IEEE Journal of Biomedical and Health Informatics, 25*(2), 493–503. https://doi.org/10.1109/JBHI.2020.3000057

Kurosu, A., Coyle, J. L., Dudik, J. M., & Sejdić, E. (2019). Detection of swallow kinematic events from acoustic high-resolution cervical auscultation signals in patients with stroke. *Archives of Physical Medicine and Rehabilitation, 100*(3), 501–508. https://doi.org/10.1016/j.apmr.2018.05.038

Lof, G. L., & Robbins, J. (1990). Test–retest variability in normal swallowing. *Dysphagia, 4*(4), 236–242. https://doi.org/10.1007/BF02407271

Loth, A., Corny, J., Santini, L., Dahan, L., Dessi, P., Adalian, P., & Fakhry, N. (2015). Analysis of hyoid–larynx complex using 3D geometric morphometrics. *Dysphagia, 30*(3), 357–364. https://doi.org/10.1007/s00455-015-9609-2

Mao, S., Sabry, A., Khalifa, Y., Coyle, J. L., & Sejdić, E. (2021). Estimation of laryngeal closure duration during swallowing without invasive X-rays. *Future Generation Computer Systems, 115,* 610–618. https://doi.org/10.1016/j.future.2020.09.040

Mao, S., Zhang, Z., Khalifa, Y., Donohue, C., Coyle, J. L., & Sejdić, E. (2019). Neck sensor-supported hyoid bone movement tracking during swallowing. *Royal Society Open Science, 6*(7), 181982. https://doi.org/10.1098/rsos.181982

Martin-Harris, B., Brodsky, M. B., Michel, Y., Castell, D. O., Schleicher, M., Sandidge, J., Maxwell, R., & Blair, J. (2008). MBS measurement tool for swallow impairments—MBSImP: Establishing a standard. *Dysphagia, 23*(4), 392–405. https://doi.org/10.1007/s00455-008-9185-9

Molfenter, S. M., & Steele, C. M. (2013). Variation in temporal measures of swallowing: Sex and volume effects. *Dysphagia, 28*(2), 226–233. https://doi.org/10.1007/s00455-012-9437-6

Molfenter, S. M., & Steele, C. M. (2014). Use of an anatomical scalar to control for sex-based size differences in measures of hyoid excursion during swallowing. *Journal of Speech, Language, and Hearing Research, 57*(3), 768–778. https://doi.org/10.1044/2014_JSLHR-S-13-0152

Onesti, E., Schettino, I., Gori, M. C., Frasca, V., Ceccanti, M., Cambieri, C., Ruoppolo, G., & Inghilleri, M. (2017). Dysphagia in amyotrophic lateral sclerosis: Impact on patient behavior, diet adaptation, and riluzole management. *Frontiers in Neurology, 8,* 94. https://doi.org/10.3389/fneur.2017.00094

Oppenheim, A. V., Schafer, R. W., & Buck, J. R. (1999). *Discrete-time signal processing* (2nd ed.). Prentice Hall.

Paris, G., Martinaud, O., Petit, A., Cuvelier, A., Hannequin, D., Roppeneck, P., & Verin, E. (2013). Oropharyngeal dysphagia in amyotrophic lateral sclerosis alters quality of life. *Journal of Oral Rehabilitation, 40*(3), 199–204. https://doi.org/10.1111/joor.12019

Plowman, E. K., Tabor-Gray, L., Rosado, K. M., Vasilopoulos, T., Robison, R., Chapin, J. L., Gaziano, J., Vu, T., & Gooch, C. (2019). Impact of expiratory strength training in amyotrophic lateral sclerosis: Results of a randomized, sham-controlled trial. *Muscle & Nerve, 59*(1), 40–46. https://doi.org/10.1002/mus.26292

Plowman, E. K., Watts, S. A., Robison, R., Tabor-Gray, L., Dion, C., Gaziano, J., Vu, T., & Gooch, C. (2016). Voluntary cough airflow differentiates safe versus unsafe swallowing in amyotrophic lateral sclerosis. *Dysphagia, 31*(3), 383–390. https://doi.org/10.1007/s00455-015-9687-1

Ramagalla, A. R., Sadanandam, P., & Rajasree, T. K. (2014). Age related metric changes in the hyoid bone. *IOSR Journal of Dental and Medical Sciences, 13*(7), 54–56. https://doi.org/10.9790/0853-13765456

Rebrion, C., Zhang, Z., Khalifa, Y., Ramadan, M., Kurosu, A., Coyle, J. L., Perera, S., & Sejdić, E. (2019). High-resolution cervical auscultation signal features reflect vertical and horizontal displacements of the hyoid bone during swallowing. *IEEE Journal of Translational Engineering in Health and Medicine, 7,* 1–9. https://doi.org/10.1109/JTEHM.2018.2881468

Robbins, J., Coyle, J., Rosenbek, J., Roecker, E., & Wood, J. (1999). Differentiation of normal and abnormal airway protection during swallowing using the penetration–aspiration scale. *Dysphagia, 14*(4), 228–232. https://doi.org/10.1007/PL00009610

Robbins, J., Hamilton, J. W., Lof, G. L., & Kempster, G. B. (1992). Oropharyngeal swallowing in normal adults of different ages. *Gastroenterology, 103*(3), 823–829. https://doi.org/10.1016/0016-5085(92)90013-O

Robison, R., Tabor-Gray, L. C., Wymer, J. P., & Plowman, E. K. (2018). Combined respiratory training in an individual with C9orf72 amyotrophic lateral sclerosis. *Annals of Clinical and Translational Neurology, 5*(9), 1134–1138. https://doi.org/10.1002/acn3.623

Sabry, A., Mahoney, A. S., Mao, S., Khalifa, Y., Sejdić, E., & Coyle, J. L. (2020). Automatic estimation of laryngeal vestibule

closure duration using high-resolution cervical auscultation signals. *Perspectives of the ASHA Special Interest Groups, 5*(6), 1647–1656. https://doi.org/10.1044/2020_PERSP-20-00073

Schwartz, D. B. (2018). Enteral nutrition and dementia integrating ethics. *Nutrition in Clinical Practice, 33*(3), 377–387. https://doi.org/10.1002/ncp.10085

Sejdić, E., Steele, C. M., & Chau, T. (2013). Classification of penetration–aspiration versus healthy swallows using dual-axis swallowing accelerometry signals in dysphagic subjects. *IEEE Transactions on Biomedical Engineering, 60*(7), 1859–1866. https://doi.org/10.1109/TBME.2013.2243730

Shrout, P. E., & Fleiss, J. L. (2005). Intraclass correlations: Uses in assessing rater reliability. *Psychological Bulletin, 86*(2), 420–428. https://doi.org/10.1037/0033-2909.86.2.420

Shu, K. (2019). *Association between diameter of upper esophageal sphincter maximal opening and high-resolution cervical auscultation signal features* [Master's thesis, University of Pittsburgh].

Shu, K., Coyle, J. L., Perera, S., Khalifa, Y., Sabry, A., & Sejdić, E. (2021). Anterior–posterior distension of maximal upper esophageal sphincter opening is correlated with high-resolution cervical auscultation signal features. *Physiological Measurement, 42*(3), Article 035002. https://doi.org/10.1088/1361-6579/abe7cb

Smith, L., & Ferguson, R. (2017). Artificial nutrition and hydration in people with late-stage dementia. *Home Healthcare Now, 35*(6), 321–325. https://doi.org/10.1097/NHH.0000000000000550

Suttrup, I., & Warnecke, T. (2016). Dysphagia in Parkinson's disease. *Dysphagia, 31*(1), 24–32. https://doi.org/10.1007/s00455-015-9671-9

Tabor-Gray, L., Rosado, K. M., Robison, R., Hegland, K. W., Humbert, I. A., & Plowman, E. K. (2016). Respiratory training in an individual with amyotrophic lateral sclerosis. *Annals of Clinical and Translational Neurology, 3*(10), 819–823. https://doi.org/10.1002/acn3.342

Takahashi, K., Groher, M. E., & Michi, K. (1994). Methodology for detecting swallowing sounds. *Dysphagia, 9*(1), 54–62. https://doi.org/10.1007/BF00262760

Troche, M. S., Okun, M. S., Rosenbek, J. C., Musson, N., Fernandez, H. H., Rodriguez, R., Romrell, J., Pitts, T., Hegland, K. W., & Sapienza, C. M. (2010). Aspiration and swallowing in Parkinson disease and rehabilitation with EMST: A randomized trial. *Neurology, 75*(21), 1912–1919. https://doi.org/10.1212/WNL.0b013e3181fef115

Waito, A. A., Plowman, E. K., Barbon, C. E. A., Peladeau-Pigeon, M., Tabor-Gray, L., Magennis, K., Robison, R., & Steele, C. M. (2020). A cross-sectional, quantitative videofluoroscopic analysis of swallowing physiology and function in individuals with amyotrophic lateral sclerosis. *Journal of Speech, Language, and Hearing Research, 63*(4), 948–962. https://doi.org/10.1044/2020_JSLHR-19-00051

Waito, A. A., Valenzano, T. J., Peladeau-Pigeon, M., & Steele, C. M. (2017). Trends in research literature describing dysphagia in motor neuron diseases (MND): A scoping review. *Dysphagia, 32*(6), 734–747. https://doi.org/10.1007/s00455-017-9819-x

Yu, C., Khalifa, Y., & Sejdić, E. (2019). Silent aspiration detection in high resolution cervical auscultations. In *2019 IEEE EMBS International Conference on Biomedical & Health Informatics (BHI)*. Institute of Electrical and Electronics Engineers. https://doi.org/10.1109/BHI.2019.8834576

Zhang, Z., Perera, S., Donohue, C., Kurosu, A., Mahoney, A. S., Coyle, J. L., & Sejdić, E. (2020). The prediction of risk of penetration–aspiration via hyoid bone displacement features. *Dysphagia, 35*(1), 66–72. https://doi.org/10.1007/s00455-019-10000-5